Optical Materials 46 (2015) 384–388

Contents lists available at ScienceDirect

Optical Materials

journal homepage: www.elsevier.com/locate/optmat

Ultra-bandwidth polarization splitter based on soft glass dual-core photonic crystal fiber

Zhenkai Fan [a,b], Shu-Guang Li [a,*], Jianshe Li [a], Zhiyi Wei [b], Wenlong Tian [b]

[a] Key Laboratory of Metastable Materials Science and Technology, College of Science, Yanshan University, Qinhuangdao 066004, PR China
[b] Laboratory of Optical Physics, Beijing National Laboratory for Condensed Matter Physics, Institute of Physics, Chinese Academy of Sciences, Beijing 100190, PR China

ARTICLE INFO

Article history:
Received 2 April 2015
Received in revised form 17 April 2015
Accepted 19 April 2015
Available online 11 May 2015

Keywords:
Dual-core photonic crystal fiber
Soft glass
Polarization splitter

ABSTRACT

A novel ultra-bandwidth polarization splitter based on soft glass dual-core photonic crystal fiber (DC-PCF) is designed in this paper, which is analyzed through the finite element method (FEM). The coupling characteristics of the designed DC-PCF can be enhanced by a high refractive index As_2S_3 core. Numerical results show the ultra-bandwidths of the *x*- and *y*-polarization modes can reach to 86 nm and 60 nm as the extinction ratios better than −20 dB and −30 dB at the vicinity of the wavelength of 1.31 μm. The length of the designed soft glass DC-PCF is 52.29 mm and the extinction ratios of the *x*- and *y*-polarization modes are −85.57 dB and −56.81 dB at the wavelength of 1.31 μm, respectively. In addition, the designed splitter has a tolerance of ±10 nm in its all structure parameters, which make the design not sensitive to the perturbation during the fabrication process.

1. Introduction

The fiber coupler plays an important role in the optical communication systems, which can transfer, divide or combine the optical power. It has been reported in Ref. [1] that it is possible to use a dual-core photonic crystal fiber (DC-PCF) as an optical fiber coupler, which has several advantage compared with conventional fiber-coupler. The PCF coupler has vast design possibilities [2], short coupling length and large index contrast. For these reasons, some research groups have proposed that the designed PCF coupler is likely to be used as a polarization splitter [3], wavelength division multiplexer [4], polarization filters [5], all-optical switching device [6] and directional coupler [7]. Saitoh et al. [8] simulated coupling characteristics of DC-PCF couplers by using the FEM and successfully applied to a multiplexer–demultiplexer (MUX–DEMUX) based on PCF. Hameed and Obayya [9] proposed and analyzed a novel polarization splitter based on index-guiding soft glass nematic liquid crystal (NLC) PCF, which can provided low crosstalk of better than −20 dB with great bandwidths of 30 nm and 75 nm for the quasi TE and TM modes.

Various types of PCF splitting-structures rely their polarization splitting performance on the coupling between the *x*-polarization and *y*-polarization modes. However, the FEM [10] has been developed to accurately calculate the modal solution of input waveguide by means of flexible triangular and curvilinear meshes. Since a new fabrication technique to define the input waveguide into silica-material PCF has been developed successfully, the polarization-dependent coupling [11] and polarization-indepen dent splitting [12] operations were implemented to use a dual-core PCF based on silica material at the 1.31 μm and 1.55 μm wavelength bands. In addition, the task to design single-polarization single-core PCF for wavelength splitter having polarization-independent propagation characteristics, and allowing wavelength multiplexing at two different wavelength bands. It was an important break-though from the design, fabrication and functionality point of view [13]. Furthermore, as the soft glass has much lower softening temperature of ∼520 °C [14] than ∼1500–1600 °C of silica glass, the extrusion approach as a practical technique has been recently extended to extrude the PCF preform directly from the bulk glass.

In this paper, we propose a novel polarization splitter based on soft glass DC-PCF. The polarization coupling properties of the *x*- and *y*-polarization modes is analyzed by the FEM. As the refractive index of SF57 is less than that of As_2S_3, the polarization dependant coupling of the designed soft glass DC-PCF is enhanced by the high index chalcogenide glass core. Numerical results show that the polarization splitting can be obtained by the coupling ratio of 2:1 for *x*- and *y*-polarization modes. From the viewpoint of fabrication, as the softening temperature of SF57 and As_2S_3 glass is almost equal, the extrusion approach as a practical technique can be used to draw the designed soft glass DC-PCF with a As_2S_3 core.

* Corresponding author.
E-mail address: shuguangli@ysu.edu.cn (S.-G. Li).

http://dx.doi.org/10.1016/j.optmat.2015.04.052
0925-3467/

2. Structure and operation principle of the polarization splitter

Fig. 1. shows the cross section of the designed splitter. All circular air holes are arranged in a triangular lattice with the lattice constant of $\Lambda = 2.2818$ μm. Two cores of A and B are formed by taking out two air holes and the eight smaller air holes with the diameters of $d_1 = 0.5$ μm are placed in around this two cores, which can enhance the birefringence property of the designed DC-PCF. The conventional holes with the diameters of $d_0 = 0.6$ μm are used to confine the energy in two cores, and the black air hole with the diameter of $d_a = 0.6$ μm is infiltrated with chalcogenide glass of As_2S_3 in the center of DC-PCF. The refractive index of the air is set as 1. So far, most of the proposed wavelength splitters [15] are based on the two core structure, and two inner cores distance is very small. In our paper, the polarized coupling of the *x*- and *y*-polarization modes is enhanced by the central high-guide rod with the As_2S_3.

The background material and the central functional material of the designed DC-PCF splitter are two types of soft glass of SF57 and As_2S_3, respectively. The refractive index of As_2S_3 is larger than that of SF57 [16], while the softening temperature of SF57 and As_2S_3 is almost equal. The material dispersion of SF57 material can be defined by the Sellmeier equation:

$$n_{SF57}(\lambda) = \sqrt{B_0 + B_1\lambda^2 + \frac{B_2}{\lambda^2} + \frac{B_3}{\lambda^4} + \frac{B_4}{\lambda^6} + \frac{B_5}{\lambda^8}} \quad (1)$$

where $n_{SF57}(\lambda)$ is the wavelength-dependent refractive index of SF57 material, $B_0 = 3.24748$, $B_1 = -0.00954782$ μm^{-2}, $B_2 = 0.0493626$ μm^2, $B_3 = 0.00294294$ μm^4, $B_4 = -1.48144 \times 10^{-4}$ μm^6, and $B_5 = 2.78427 \times 10^{-5}$ μm^8. The Sellmeier equation of the Chalcogenide glass is given by [17]:

$$n_{As_2S_3}(\lambda) = \sqrt{1 + \sum \frac{A_i\lambda^2}{\lambda^2 - C_i^2}} \quad (2)$$

where $i = 5$, $A_1 = 1.898367$, $A_2 = 1.922297$, $A_4 = 0.87651$, $A_5 = 0.95699$, $C_1 = 0.15$ μm, $C_2 = 0.25$ μm, $C_3 = 0.35$ μm, $C_4 = 0.45$ μm and $C_5 = 27.3861$ μm.

3. Numerical results and analysis

The electric field distributions of four guided modes of the designed DC-PCF at the operating wavelength of 1.31 μm are shown in Fig. 2. The mode formed on the high refractive-index rod can be provided in this simulation, which is very similar with the 2nd-order SPP mode formed on the surface of the metallic gold from Ref. [18]. It is a major discovery that this mode can occur on surface of high refractive index of As_2S_3 rod. From Fig. 2(b) and (d), we can observe that the phase matching between the mode on the rod and the odd core-guided modes can be satisfied, the energy of the core-guided odd mode can couple into the surface of the high-index rod. However, Fig. 2(a) and (c) shows the phase matching between the mode on the rod and the odd core-guided modes in *x*- and *y*-polarization is not met at the operating wavelength of 1.31 μm.

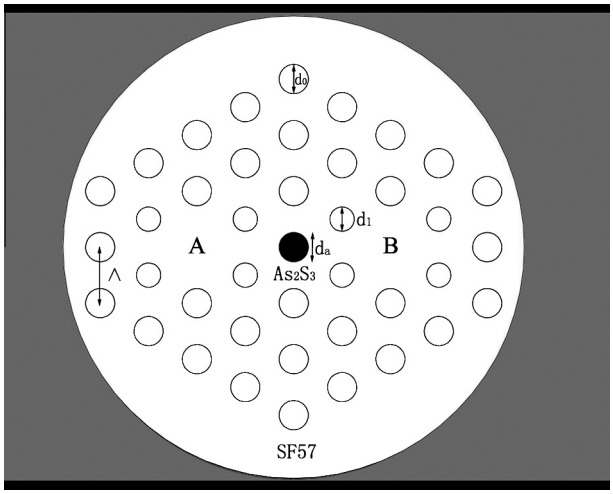

Fig. 1. Cross section of the designed soft glass DC-PCF splitter with a As_2S_3 core.

The coupling length, defined as the minimum fiber distance where the maximum power transfer occurs between two cores, is considered as one of the key characteristics of the directional coupler. The refractive indexes of the *x*, *y*-odd and even modes of the design DC-PCF are evaluated by the FEM. The perfect matched layer with several micrometer is set in the outmost layer, which can reduce the numerical error. Coupling length L_C can be calculated by Eq. (3).

$$L_C = \frac{\lambda}{2(n_{even}^{x,y} - n_{odd}^{x,y})} \quad (3)$$

Fig. 3 shows the coupling lengths and coupling ratios of *x*- and *y*-polarization modes as functions of the hole pitch of Λ for the designed soft glass DC-PCF with a As_2S_3 core and conventional soft glass DC-PCF at the operating wavelength of 1.31 μm. It is very obvious that the designed soft glass DC-PCF is always shorter than that of conventional soft glass DC-PCF. As shown in Fig. 3, the coupling lengths of *x*- and *y*-polarization modes of the conventional soft glass DC-PCF shows monotonic decrease with the increasing of Λ, but the coupling ratio maintains a low value of about 1.30. However, due to introducing a high refractive index of As_2S_3 core which increases the birefringence between *x*-polarization mode and *y*-polarization mode, and polarization dependence of the designed soft glass DC-PCF with a As_2S_3 core is enhanced. Therefore, the coupling lengths of the designed soft glass DC-PCF with a As_2S_3 core shows an increasing trend with the increasing of the hole pitch of Λ, although the coupling lengths is much shorter than that of the conventional soft glass DC-PCF. The coupling ratio of designed soft glass DC-PCF with the As_2S_3 core can reach to the optimal of 2, when the stature parameters are the diameters of $d_0 = 0.6$ μm, $d_a = 0.6$ μm and $d_1 = 0.5$ μm and the hole pitch of $\Lambda = 2.2818$ μm.

In order to achieve a polarization splitter based on the soft glass DC-PCF with a As_2S_3 core, the beam propagation method (BPM) is used to research the transmission characteristics along this fiber. Initially, at the propagation distance of $Z = 0$ μm, a beam polarization light achieved using the FVFDM [19] at the wavelength of 1.31 μm are launched into the left core A of this designed DC-PCF, the *x*- and *y*-polarization modes can be separated along the fiber transmitted over a fixed length. Fig. 4 shows the variation of normalized powers of the *x*- and *y*-polarization modes for the left core A and the right core B at the operating wavelength of 1.31 μm, respectively. It is obvious from Fig. 4 that the *x*- and the *y*-polarization modes can be separated well into the core A and core B after a propagation distance of $Z = 52.29$ mm. As shown in Fig. 5, the normalized powers of the *x*- and *y*-polarization modes at core A and core B as periodic function of the propagation distance at the wavelength of 1.31 μm for the conventional soft glass DC-PCF, respectively. It is very obvious that the *x*- and *y*-polarization modes can be separated well into the two core A and core B, respectively, when the propagation distance is 1148 mm.

The impact of chalcogenide glass core on the performance of the polarization splitter is further studied by comparing with the conventional soft glass DC-PCF polarization splitter. The fiber

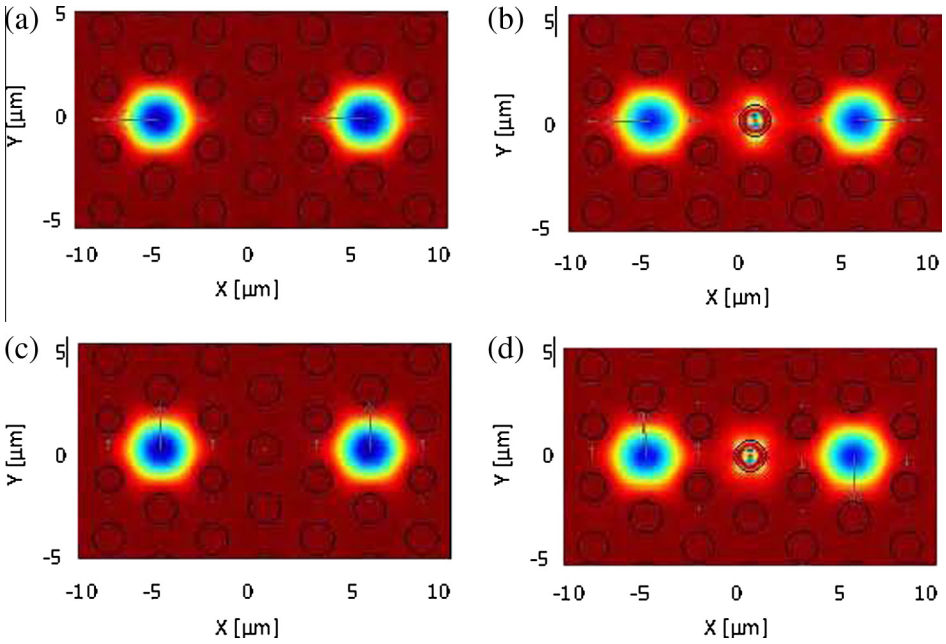

Fig. 2. The electric field distributions of four super modes of the designed DC-PCF at the operating wavelength of 1.31 μm. (a) Even mode in the *x* polarization, (b) odd mode in *x*-polarization, (c) even mode in *y*-polarization, and (d) odd mode in *y*-polarization.

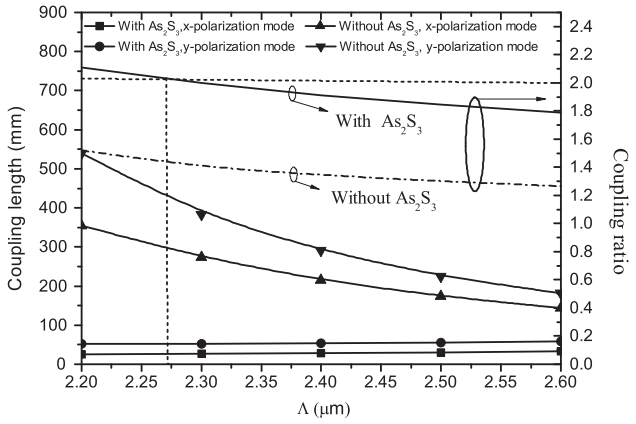

Fig. 3. The coupling lengths and coupling ratios of *x*- and *y*-polarization modes as functions of the hole pitch of Λ for the designed soft glass DC-PCF with a As_2S_3 core and the conventional soft glass DC-PCF.

polarization splitter can separate the two orthogonal polarized states of *x*- and *y*-polarization modes at a given wavelength, if the coupling length of the *x*- and *y*-polarization modes can meet the coupling length ratio:

$$R = L_Y : L_X = m : n \tag{4}$$

where *m* and *n* are the integers of different parities, and the length of the splitter can be represented by $L_{\text{fiber}} = L_x \times \frac{m}{n}$. Therefore, the shortest splitter is achieved, when the coupling ratio of *R* is optimized to 2.

Fig. 6. shows the coupling length and coupling ratio of the *x*- and *y*-polarization modes as function of wavelength in the designed soft glass DC-PCF with a As_2S_3 core and the conventional soft glass DC-PCF, when the hole pitch of the designed DC-PCF with a As_2S_3 core and the conventional soft glass DC-PCF are 2.2818 μm. It is observed that the coupling length of *x*- and *y*-polarization modes of the designed soft glass DC-PCF with a As_2S_3 core is much shorter than that of the conventional soft glass DC-PCF, while the coupling ratio of the designed soft glass DC-PCF with a As_2S_3 core is higher than that of the conventional soft glass DC-PCF. Furthermore, the coupling characteristics can be meaningful changed by the higher refractive index of chalcogenide glass core, and the coupling ratio is meaningful increased to 2 by the enhanced birefringence.

The extinction ratio (ER) is a key technology parameter of the polarization splitter, which can characterize the quality of splitting performance. The extinction ratios around the operating wavelength of 1.31 μm of the *x*- and *y*-polarization modes for the designed soft glass DC-PCF and the conventional soft glass DC-PCF are shown in Figs. 7 and 8, respectively. The ER of the desired *x*-polarization mode at the left core A is defined as:

$$\text{ER}_X = -10\log 10\left(\frac{P_{dX}^A}{P_{uY}^A}\right) \tag{5}$$

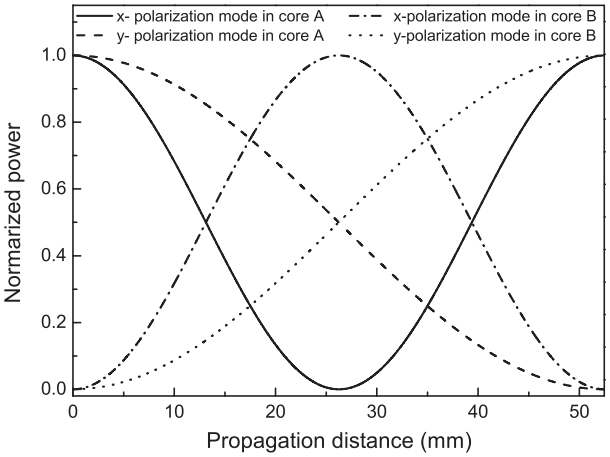

Fig. 4. Variation of normalized powers of *x*- and *y*-polarization modes in core A and B along the propagation distance at the operating wavelength of 1.31 μm for the designed soft glass DC-PCF with the As_2S_3 core.

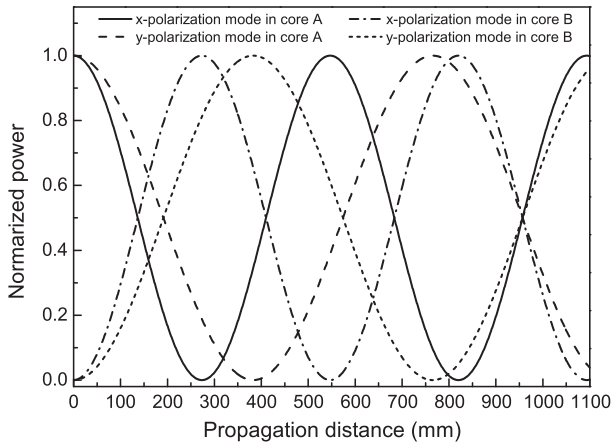

Fig. 5. Variation of normalized powers of *x*- and *y*-polarization modes in core A and B along the propagation distance at the operating wavelength of 1.31 μm for the conventional soft glass DC-PCF.

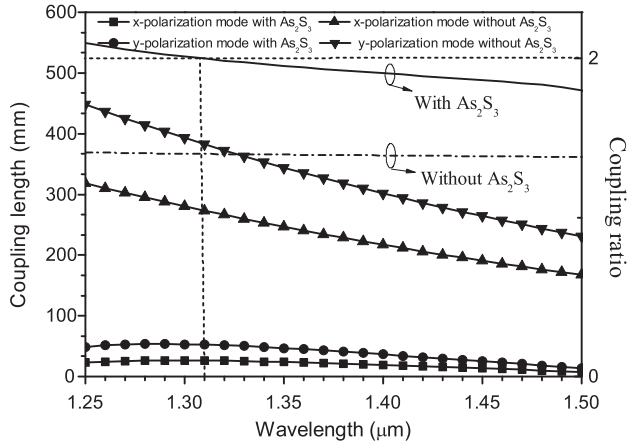

Fig. 6. Various of coupling lengths of the *x*- and *y*-polarization modes for the designed DC-PCF with a As_2S_3 core and the conventional soft glass DC-PCF with the wavelength.

where P^A_{dX} and P^A_{uY} are the normalized powers of the desired *x*-polarization mode and the unwanted *y*-polarization mode in the left core A, respectively. Furthermore, the extinction ratio of the *y*-polarization mode in the right core B is expressed by:

$$\mathrm{ER}_Y = -10\log 10\left(\frac{P^B_{dY}}{P^B_{uX}}\right) \tag{6}$$

where P^B_{dY} and P^B_{uX} represent the normalized power of the desired *y*-polarization mode and the unwanted *x*-polarization mode at core B, respectively. As shown in Fig. 7, the designed soft glass polarization splitter with a As_2S_3 core has large bandwidths of 86 nm and 60 nm for the *x*- and *y*-polarization modes, respectively, where the extinction ratio is better than −20 dB and −30 dB. We can see that the bandwidths of *x*- and the *y*-polarization modes are almost equal, and the extinction ratios of the *x*- and *y*-polarization modes are −85.57 dB and −56.81 dB at the wavelength of 1.31 μm, respectively. However, it is revealed from Fig. 8 that bandwidths of the *x*- and *y*-polarization modes for the conventional soft glass polarization splitter are 42 nm and 49 nm, the extinction ratio is better than −10 dB, respectively, and the bandwidths of the *x*- and *y*-polarization modes are very inconsistent. Furthermore, the splitting performance of the designed soft glass polarization splitter with the As_2S_3 core is far better than the conventional soft glass polarization splitter.

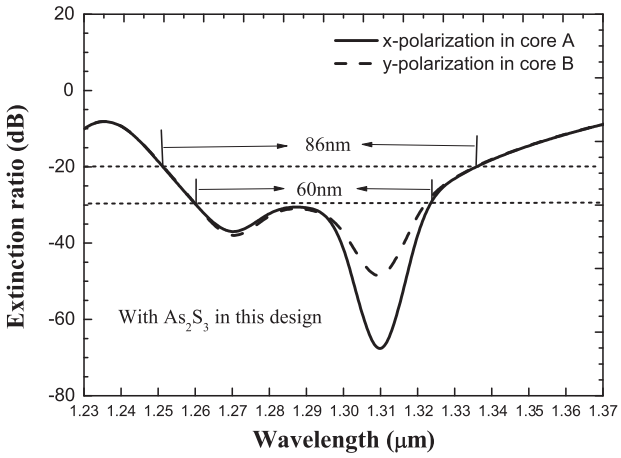

Fig. 7. Various of extinction ratios of *x*- and *y*-polarization modes in the designed DC-PCF with a As_2S_3 core.

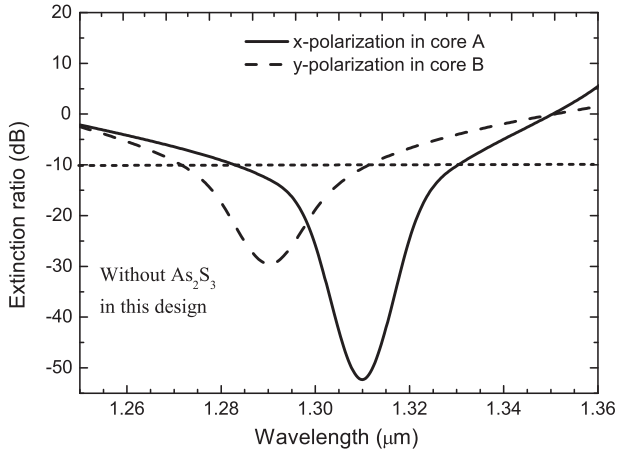

Fig. 8. Various of extinction ratios of *x*- and *y*-polarization modes in the conventional soft glass DC-PCF.

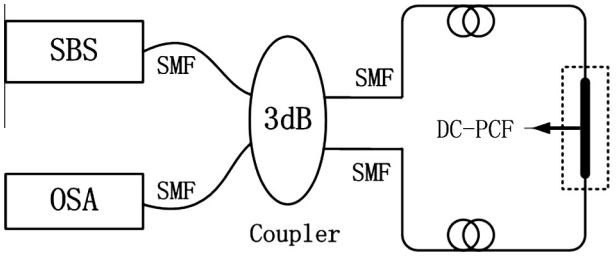

Fig. 9. The schematic diagram of polarization splitting system.

Fig. 9 shows the schematic diagram of the designed polarization splitter system based on DC-PCF with the As_2S_3 core. The designed sensing system is composed of a supercontinuum broadband source (SBS), a 3 dB coupler, a designed soft glass DC-PCF with the As_2S_3 core, and an optical spectrum analyzer (OSA). The single mode fiber (SMF) is used to connect the components of the splitting system. The SBS is used to launch light into this system, and the back reflected spectrum shifts were detected by this OSA.

The tolerance of Λ_0, d_0, d_1 and d_a for realistic fabrication has been analyzed in Fig.10. We investigate the impact of the slight changes in Λ, d_0, d_1 and d_a of ±10 nm on the extinction ratio of

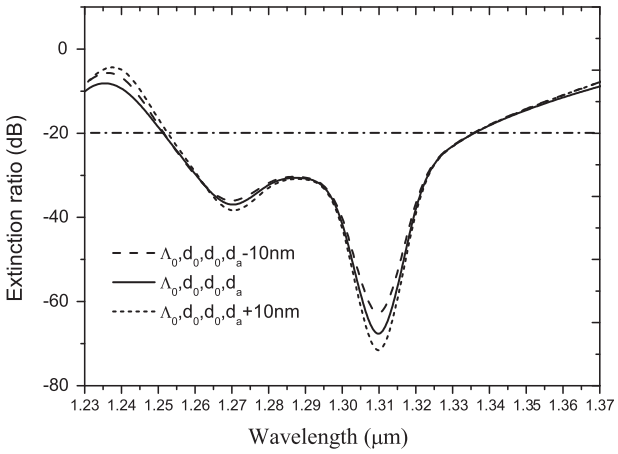

Fig. 10. The extinction ratio with different fabrication tolerance of Λ.

the designed soft glass polarization splitter with a As_2S_3 core, and the optimization hole pitch of Λ_0 is 2.2818 μm. As shown in Fig. 10, numerical simulations reveals that the designed soft glass polarization splitter with a As_2S_3 core possesses a relative stable realistic fabrication tolerance.

4. Conclusion

We propose a novel ultra-bandwidth polarization splitter based on soft glass dual-core photonic crystal fiber in this paper. These results are evaluated by using the FEM and BPM. It is obviously observed that the high refractive index of the As_2S_3 core can promote the polarization dependent coupling of *x*- and *y*-polarization modes between the left core A and the right core B. The coupling lengths of two polarization states are reduced by the enhanced birefringence. For the designed 52.29-mm-long polarization splitter, numerical results show the ultra-bandwidths of *x*- and *y*-polarization modes around the wavelength of 1.31 μm are 86 nm and 60 nm, as the extinction ratio better than −20 dB and −30 dB, respectively while the bandwidths of *x*- and *y*-polarization modes are almost consistent. Besides, the tolerance of ±10 nm in all structure parameters is investigated for the designed polarization splitter, which reveals that this designed polarization splitter is not sensitive to slight changes during realistic fabrication process.

Acknowledgements

This work was supported by the National Natural Science Foundation of China (Grant Nos. 61178026 and 61475134) and the Nature Science Foundation of Hebei Province, China (Grant No. E2012203035).

References

[1] H.W. Lee, Appl. Phys. Lett. 93 (2008) 111102.
[2] L. Zhang, C. Yang, J. Lightwave Technol. 22 (2004) 1367.
[3] L. Zhang, C. Yang, IEEE. Photon. Technol. Lett. 16 (2004) 1670.
[4] P. Geng, W. Zhang, S. Gao, S. Zhang, H. Zhang, J. Ruan, IEEE Photon. Technol. Lett. 24 (2012) 1304.
[5] J. Xue, S. Li, Y. Xiao, W. Qin, X. Xin, X. Zhu, Opt. Express 21 (2013) 13733.
[6] S.M. Hendrickson, C.N. Weiler, R.M. Camacho, P.T. Rakich, A.I. Young, M.J. Shaw, T.B. Pittman, J.D. Franson, B.C. Jacobs, Phys. Rev. A 87 (2013) 023808.
[7] Z. Zhang, Y. Tsuji, M. Eguchi, IEEE Photon. Technol. Lett. 26 (2014) 541.
[8] K. Saitoh, Y. Sato, M. Koshiba, Opt. Express 11 (2003) 3188.
[9] M.F.O. Hameed, S.S.A. Obayya, IEEE Photon. J. 1 (2009) 265.
[10] L.J. Armitage, M.B. Doost, W. Langbein, E.A. Muljarov, Phys. Rev. A 89 (2014) 053832.
[11] B. Sun, M. Chen, J. Zhou, K. Zhang, Plasmonics 8 (2013) 1253.
[12] S. Zhang, X. Yu, P. Shum, Y. Zhang, L. Xia, D. Liu, IEEE Photon. J. 4 (2012) 1178.
[13] W.E.P. Padden, M.A. van Eijkelenborg, A. Argyros, N.A. Issa, Appl. Phys. Lett. 84 (2004) 1689.
[14] M.F.O. Hameed, S.S.A. Obayya, IEEE J. Quantum Electron. 47 (2011) 1283.
[15] K. Saitoh, Y. Sato, M. Koshiba, Opt. Express 12 (2004) 3940.
[16] M.F.O. Hameed, A.M. Heikal, S.S.A. Obbayya, IEEE Photon. Technol. Lett. 25 (2013) 1578.
[17] E. Nazemosadat, A. Mafi, Opt. Lett. 39 (2014) 4675.
[18] P. Li, J.L. Zhao, Opt. Express 21 (2013) 5232.
[19] M.F.O. Hameed, S.S.A. Obayya, Opt. Lett. 39 (2014) 1077.